# Adsorption of Mercury by *Pterocarpus Anglolensis*: Study on Adsorption Isotherms and Kinetics

**Mapombere, Garainesu; Nyoni, Bothwell**

*Department of Applied Chemistry, National University of Science and Technology, Bulawayo, ZIMBABWE*

**Sibali, Linda L.**

*Department of Environmental Sciences, College of Agriculture and Environmental Sciences,*
*University of South Africa, Florida, SOUTH AFRICA*

**Chiririwa, Haleden\*[+]; Seodigeng, Tumisang**

*Department of Chemical Engineering, Vaal University of Technology, Private Bag X021, Vanderbijlpark, 1911,*
*Andries Potgieter Blvd, SOUTH AFRICA*

**ABSTRACT:** *The efficiency of Pterocarpus Anglolensis sawdust, an abundantly available waste product of the timber industry, capacity as an adsorbent for mercury was investigated. A series of batch experiments was carried out with experimental conditions of metal concentration, adsorbent concentration, pH, and contact time being changed. The concentration of the metal ion was deduced using spectrophotometric means. The adsorption efficiency was found to be pH-dependent with pH 4 being the optimum. 90 minutes was found to be the equilibrium time with particle size range 90-124 μm being the most efficient. Maximum adsorption of mercury was evaluated at 80.33 %. The experimental data was best modeled by the Freundlich isotherm and Pseudo second-order kinetic models. The calculated adsorption parameters are $K_f = 0.0002$ L/mg, $b_F = 3.0$ and $k_2 = 0.00016$ g/μg.min.*

**KEYWORDS:** *Adsorption; Pterocarpus Anglolensis; Isotherms; Kinetics.*

## INTRODUCTION

Due to natural and production activities, mercury contamination has become one of the major environmental problems over the world. Mercury contamination is a serious threat to human health [1]. The use of low cost abundantly available material to purify water of heavy metals has over the years received a lot of attention. This is due to the cost benefits associated with these adsorbents as well as the environmental friendliness aligned with their use [2].

Mercury in the mining industry is used for amalgamation purposes so as to achieve the separation of fine gold particles. The amalgamation step results in the formation of Au-Hg complex which is separated by heating and releases Hg into the atmosphere [3]. A lot of mercury is also lost in the rivers through handling errors as well as volatilization. Mercury tailings that are left in the mining sites also contribute significantly to the amount of mercury discharged into the environment

during mining [4]. Generally, the metal exists in three forms, elementary mercury, $Hg^0$, inorganic mercury, $Hg^{2+}$ salts, and organo-mercury, with the most prevalent form being methyl mercury [5]. The presence of these species of mercury in the environment is interchangeable. From gravimetric material flow analyses, it was shown that 70-80 % of the mercury is lost to the atmosphere during the processing of gold while 20-30 % is lost to tailings, soils, stream sediments, and water. For every 1 g of gold produced, 1.2 - 1.5 g of mercury is lost to the environment [6].

Organic methylmercury ($CH_3Hg$) is linked to high bioaccumulation in food chains [7–9]. Human beings accumulate mercury by the consumption of plants or fish contaminated with methylmercury. Mercury causes a host of health effects in the body. These include, most critically, a deterioration of the nervous system, impaired vision, speech and gait, involuntary movement of muscles, corroded skin and mucus membranes as well as difficulty in chewing and swallowing [10].

To deal with the increasingly serious mercury pollution, a number of methods have been investigated for the removal of $Hg^{2+}$ i.e. chemical precipitation, ion exchange, adsorption, and ultrafiltration, to name a few [11–15]. Chemical precipitation is considered one of the widely used methods, however, it has disadvantages associated with sludge formation and disposal [16]. *Matlock et al.* [17] studied the chemical precipitation of lead and mercury by the use of ligand, 1,3 benzendiamidoethanethiol (BDETH$_2$). Removal efficiencies of 99 % and above were reported. On the other hand, *Chiarle et al.* [18] managed to demonstrate the use of ion-exchange resins to remove mercury from contaminated water using polystyrene/divinylbenzene resin with thiol functional groups. Ultrafiltration is commonly used in the removal of suspended solids and micro-organisms in water. However, it is an expensive method that is not popular with large-scale mercury removal from water. *Zambrano et al.* [19] studied the removal of mercury from aqueous solutions by a combination of complexation and ultrafiltration. Polyethylenimine was used as a complexing agent, followed by membrane separation. Mercury retention values close to 100 % were reported.

Adsorption has been the focus of research on the remediation of mercury pollution because of its simplicity. Adsorption and ion exchange share a number of similarities although ion exchange is a more complex process. Physical and chemical adsorption processes are the two major mechanisms of adsorption used for the removal of heavy metal ions from aqueous solutions. The current research effort in adsorption and ion exchange is aimed at the analysis of a variety of adsorption materials that are porous and with large surface areas [20]. Adsorption is considered the most promising technique due to its simplicity, selectivity, high efficiency, low cost, and operational convenience [21]. The use of activated carbon, magnetic materials, clay minerals, biomaterials, carbon nanotubes, and zeolites as adsorbents or ion exchange resins has been studied by a number of researchers [16, 18, 22-24]. However, the use of low-cost alternative adsorbents has gained popularity with a number of researchers. These low-cost alternative adsorbents are natural materials such as wood, peat, coal, and lignite or industrial/agricultural/domestic wastes such as slag, sludge, fly ash, bagasse fly-ash, and red mud [25]. In this work, the use of a low-cost natural adsorbent is investigated. *Pterocarpus Anglolensis* sawdust is assessed in the removal of mercury from contaminated water samples. The factors affecting the adsorption process e.g. solution pH, contact time, solution initial concentration, and adsorbent dosage are examined. The majority of studies have analyzed linear adsorption isotherms and kinetics. However, this study is unique in the sense that it seeks a deeper understanding of the isotherms and kinetics of adsorption of mercury onto *Pterocarpus Anglolensis* sawdust by evaluating and comparing results obtained via both linear and non-linear methods.

## EXPERIMENTAL SECTION

The investigation was carried out in batch experiments. All other factors were kept constant while the factor in question was varied. Every factor in question was run thrice for each set of constant factors and all experiments were carried out at room temperature.

### *Materials and methods*

*Pterocarpus anglolensis* sawdust was collected from a local timber mill. It was washed with de-ionized water and left to air dry for 48 hrs. The sawdust was homogenized by crushing in a blender and acid-treated by leaving it in 0.3 M $HNO_3$ overnight. It was washed with de-ionized water until a pH of 7 was obtained and air-dried for 48 h. A micro-millimeter sieve was used to separate the sawdust

into a fine mesh and divided into four classes of fine sawdust; 180-249 μm, 125-179 μm, 90-124 μm and < 90 μm. The four sizes were treated with 2 M NaOH overnight followed by final washing and dried in air for 48 h Mercuric Chloride (analytical grade) was purchased from Sigma Aldrich. The working solutions were prepared from the stock solutions by dilution to the desired concentration. Mercury concentration was determined °C by using a UV/Vis spectrophotometer (Perkin Elmer Lambda 2) *via* a complexation method using potassium iodide and rhodamine.

### Batch equilibrium study

All experiments were performed using a rotary shaker set at a fixed speed of 160 rpm. The adsorption isotherm experiment was carried out in a batch process using 250 mL flasks. A known mass (0.2 - 0.8g) of adsorbent was added to 100 mL metal-containing solution. The mixtures were agitated for 2 h since the initial experiments managed to show that equilibrium was attained within that time frame. The equilibrium concentrations of $Hg^{2+}$ in each sample were determined using a UV/Vis Spectrophotometer after filtration.

The effect of particle size was investigated according to the following; 100 μg/l mercury solution was prepared and divided into jars each getting 50 mL. The pH of each solution was adjusted to 7. A mass of 0.5 g of adsorbent was obtained from each particle size and added to the jars labeled with the respective particle sizes of 180-249, 125-179, 90-124, and < 90 μm. The jars were shaken on a rotary shaker for 15 minutes. 50 mL solutions were filtered into 100 mL amber bottles and samples were then developed for UV/VIS analysis.

The effect of contact time was investigated by adding 50 mL of solution into 24 jars. 0.5 g of adsorbent was added to each solution and adjusted to a neutral pH of 7. The 24 flasks were shaken on a rotary shaker and removed after 15-minute intervals. Test solutions were filtered and quantified for mercury.

The effect of pH was investigated using pH values ranging from 1 to 10 at room temperature. The pH was adjusted by using 1.0 M HCl and 1.0 M NaOH. The mass of adsorbent used was 0.5 g while the concentration of mercury was 100 μg/L. The test solutions were allowed to shake until they reached an equilibrium time. The solutions were filtered and then quantified for mercury.

The effect of adsorbent concentration was investigated by varying masses of adsorbent 0.2 g to 1.6 g to 24 flasks respectively. 100 μg/L of mercury in 50 mL solution was added to the flasks with pH being adjusted to the optimum pH investigated. The solutions were shaken to equilibrium time, filtered and mercury concentration determined.

The effect of metal concentration was studied by using an optimum adsorbent mass and pH of 1 g and 4 respectively, with equilibrium time not exceeding 90 min. The particle size used was 90 – 124 μm.  Four test concentrations of mercury were used. The metal concentration varied from 50 - 150 μg/L. Each metal concentration was varied thrice for a single duration of time and time was varied in intervals of 30 – 90 minutes. After shaking the mercury concentration was determined.

### Analysis of experimental data

The amount of metal adsorbed by the adsorbent at equilibrium ($q_e$) and the percentage removal were calculated according to Eqs. (1) and (2) respectively.

$$q_e = \frac{V(C_i - C_e)}{M} \tag{1}$$

$$Removal(\%) = \frac{(C_i - C_e)}{C_i} \times 100 \tag{2}$$

Where $C_i$ and $C_e$ are the initial and equilibrium concentrations in ppm of the metal ions respectively, $V$ is the volume in liters of the solution and $M$ is the mass in grams of the adsorbent.

Data generated from experiments were fitted into linear and non-linear plots for adsorption isotherms and kinetics according to the equations shown in Table 1 [22, 26]. A number of commercial software packages such as OriginPro™, Statistica™, Matlab™, and SPSS™ can be used to fit experimental data into mathematical models by setting a default objective function [27-29]. However, a robust, more economic, and user-friendly method based on iterative non-linear least-squares regression analysis was presented by *Hossain et al.* [24]. Therefore, for this work, experimental data will be fitted using the method presented by *Hossain et al.* [24].

Where $q_t$ (μg/g) is the amount adsorbed per given time, $q_e$ (μg/g) is adsorption at equilibrium, $k_1$ (min$^{-1}$) is the pseudo-first-order rate constant, $k_2$ is the pseudo-second-order rate constant (g/μg.min), $C_e$ (μg/L) is the aqueous

*Table 1: Adsorption models for analysing experimental data.*

| | Type | Plot (y vs x) | Constants |
|---|---|---|---|
| **Isortherm models** | | | |
| **Langmuir** | | | |
| $\frac{1}{q_e} = \frac{1}{K_L C_e} + \frac{a_L}{K_L}$ | Linear | $\frac{1}{q_e}$ vs $\frac{1}{C_e}$ | $K_L(L/\mu g)$ $a_L$ $(L/\mu g)$ |
| $q_e = \frac{K_L C_e}{1 + a_L C_e}$ | Non-linear | $q_e$ vs $C_e$ | |
| **Freundlich** | | | |
| $\log q_e = b_F \log C_e + \log K_F$ | Linear | $\log q_e$ vs $\log C_e$ | $K_F(L/g)$ $b_F$(dimensionless) |
| $q_e = K_F C_e^{b_F}$ | Non-linear | $q_e$ vs $C_e$ | |
| **Kinetic models** | | | |
| **Pseudo first order** | | | |
| $\ln(q_e - q_t) = \ln q_e - k_1 t$ | Linear | $\ln(q_e - q_t)$ vs t | $k_1$(min$^{-1}$) |
| $q_t = q_e - e^{-k_1 t}$ | Non-linear | $q_t$ vs t | |
| **Pseudo second order** | | | |
| $\frac{t}{q_t} = \frac{1}{k_2 q_e^2} + \frac{1}{q_e} t$ | Linear | $\frac{t}{q_t}$ vs t | $k_2$ (g/$\mu$g.min) |
| $q_t = \frac{k_2 q_e^2 t}{1 + k_2 q_e t}$ | Non-linear | $q_t$ vs t | |

concentration at equilibrium, $K_F$ (L/mg) reflects the adsorbent capacity, $b_F$ is the heterogeneity factor, $K_L$ (L/mg) reflects the solute absorptivity, $a_L$ (L/$\mu$g) is related to the energy of adsorption.

## RESULTS AND DISCUSSION

### *Effect of process parameters on the adsorption*

*Particle size and contact time*

Fig. 1 shows the percentage adsorption of mercury with varying particle sizes with differing contact times. The general trend shows an increase in percentage adsorption with a decrease in particle size. Four particle sizes of 180-249 μm, 125-179 μm, 90-124 μm, and < 90 μm were tested giving maximum percentage adsorption of 44.11, 55.62, 81.01, and 72.18 respectively.

An adsorbent material made of particles with a smaller diameter poses a large surface area for adsorption [30]. From the four-particle size ranges investigated, the results showed that particle range 90 to 124 μm had the highest adsorption range. This is contrary to theory as it was expected that particle range < 90 μm, the smallest, would be the most efficient. However, studies conducted have shown that particle size 105-106 μm was optimum for adsorption when using sawdust adsorbents [31-33]. Smaller particle
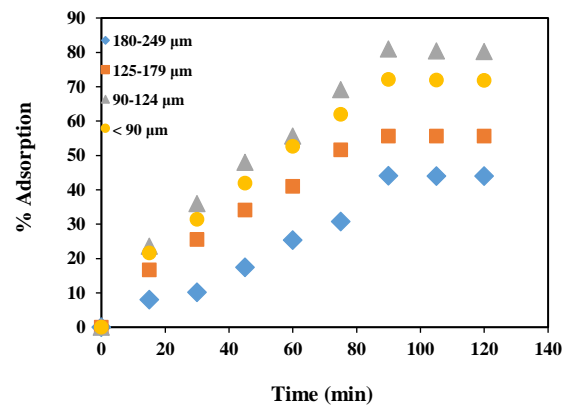


*Fig. 1: Effect of particle size and contact time on adsorption of mercury onto Pterocarpus Anglolensis [Agitation = 160 rpm, pH = 7, Adsorbent mass = 0.5 g].*

sizes tend to be light and less dense than water thus not covering the whole solution. Therefore small adsorbent particles have a high likelihood of being affected by mechanical processes. Maximum adsorption percentage was achieved for the 90 - 124 μm size at 81.01 %.

*pH*

Fig. 2 shows the percentage adsorption against pH. Increasing pH from 1 – 4, increases adsorption from

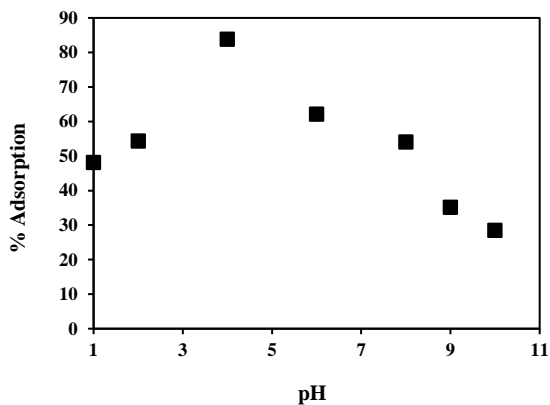*Fig. 2: Effect of pH on adsorption of mercury onto Pterocarpus Anglolensis [Agitation = 160 rpm, $C_i$ = 100 μg/L, Adsorbent mass = 0.5 g].*



*Fig. 3: Effect of adsorbent dosage on adsorption of mercury onto Pterocarpus Anglolensis [Agitation = 160 rpm, pH = 4, $C_i$ = 100 μg/L].*

48.12 % to 83.77 %. Beyond pH 4 adsorption decreases with pH values of 9 and 10 giving low adsorption values of 35.17 and 28.44 % respectively.

It is clear from Fig. 2 that the optimum pH for the adsorption of mercury on *Pterocarpus Anglolensis* sawdust is 4. Generally, the adsorption process is favorable under low pH values. Organic biomass such as sawdust is affected by pH. At particular pH values, the adsorbent assumes a charge [34, 35]. It is this charge that then affects the mercuric species present in the solution to be either attracted to the adsorbent or to be repulsive. The trend displayed in Fig. 2 indicates that at pH 4 the adsorbent assumes a positive charge. The species available in solution ($HgCl_2$) and ($HgCl_3$)$^-$ are thus more attracted to the adsorbent. Beyond this pH the adsorption capacity decreases as the adsorbent approaches the point of zero charges, which is close to neutrality. Beyond pH 7 the adsorption drops significantly. This is because the charge becomes negative, creating a repulsive force to ($HgCl_2$) and ($HgCl_3$)$^-$ species.

*Adsorbent concentration (dosage)*

Fig. 3 shows the relationship between the percentage adsorption of mercury and the mass of the adsorbent. An increase in mass of adsorbent from 0.2 g to 0.8 g results in an increase in adsorption. There is little or no change in adsorption efficiency after a dosage of 1.0 g. The maximum adsorption is 86.15 %.

The percent removal of mercury increases with an increasing amount of adsorbent. This result is an indication that the number of adsorption sites increases by increasing
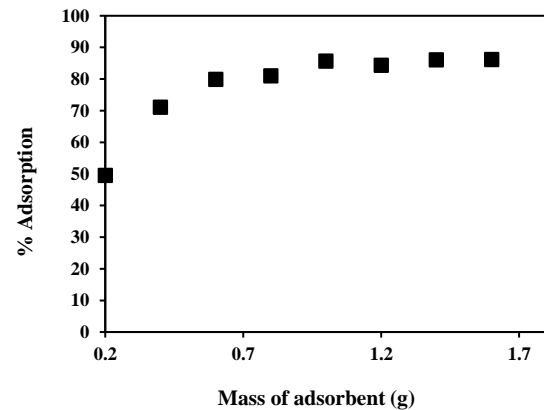
the amount of adsorbent. There was a slow increase in adsorption beyond 1 g, as the amount of metal concentration was becoming a limiting factor. These observations are in agreement with previous studies conducted using *Pterygota Macrocarpa* sawdust for adsorption of lead [36]. The conclusion was that adsorption sites are directly proportional to the amount of adsorbent. Fig. 3 shows that as a mass of the adsorbent is increased from 0.2 g to 0.8 g adsorption of the metal increases. Under the given metal concentration of 100 μg/L a mass of 1.0 g and beyond cannot achieve a further increase in adsorption than 86.15 %.

*Metal concentration and contact time*

Fig. 4 shows the effect of metal concentration and contact time on the adsorption process. An increase in metal concentration in solution leads to an increase in adsorption until no further adsorption can occur. The highest percentage adsorption of 80.23 % was achieved for a metal concentration of 150 μg/L at 120 min. For 120, 100, and 50 μg/L the percentage adsorption was 77.35, 75.03, and 62.14 respectively.

An increase in mercury ion adsorption is proportional to an increase in initial metal concentration. Therefore the greater the concentration of metal ion initially induced the greater the adsorption rate. The initial concentration provides an important driving force to overcome all mass transfer resistance of the adsorbates between the aqueous and solid phases. The equilibrium time of adsorption does not get affected by the initial concentration of the metal ion. This observation is consistent with the literature,
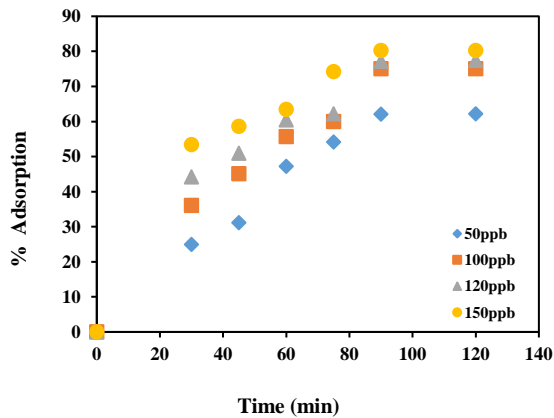
*Fig. 4: Effect of mercury concentration and contact time on adsorption onto Pterocarpus Anglolensis [Agitation = 160 rpm, pH = 4, Particle size = 90 – 124 µm, Adsorbent mass = 1 g].*



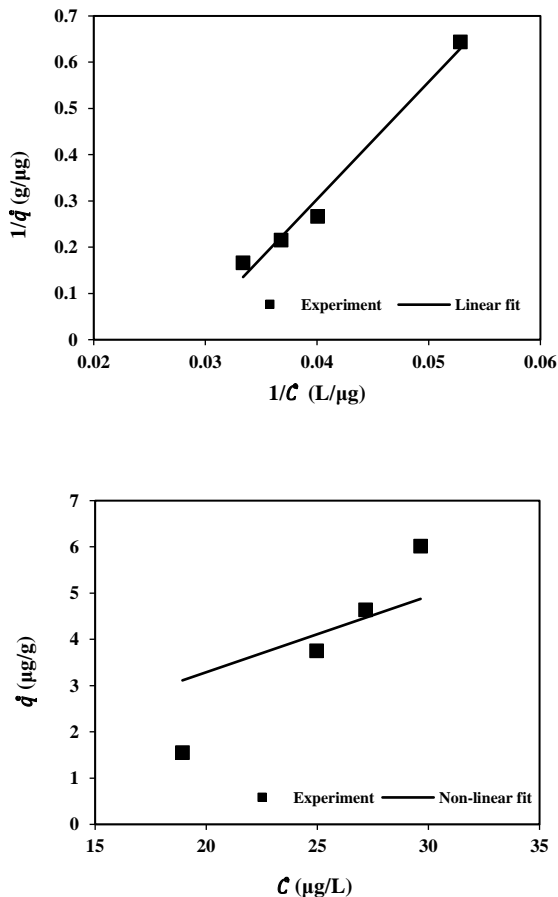*Fig. 5: Langmuir plots for adsorption of mercury onto Pterocarpus Anglolensis [Agitation = 160 rpm, pH = 4, Particle size = 90 – 124 µm, Adsorbent mass = 1 g].*

an unmodified and carboxy-methylated Granular Activated Carbon (GAC) was used to adsorb mercury and nickel from water, and it was reported that a higher concentration of metal ion resulted in higher adsorption efficiency [37].

**Adsorption isotherms**

The experimental data were fitted into Langmuir and Freundlich models according to plots presented in Table 1. These models and more have been widely used to describe metal ion adsorption processes [38–40].

The Langmuir isotherm was developed based on the assumption that each site can accommodate only one molecule of the adsorbate with no molecule migration and the energy of adsorption is constant all over the surface [41]. The maximum adsorption occurs when the monolayer of adsorbate molecules becomes saturated on the adsorbent surface and has constant energy of adsorption. The linear and non-linear forms of the model are given in Table 1. Langmuir's linear and non-linear fits are shown in Fig. 5.

The Freundlich isotherm was developed so as to model the multilayer adsorption on heterogeneous surfaces [42]. It is assumed that there is non-uniform distribution of adsorption heat and affinities over the heterogeneous surface [26]. The linear and non-linear forms of the model are given in Table 1. Fig. 6 shows the Freundlich linear and non-linear fits.

The parameters of the Langmuir and Freundlich isotherms are given in Table 2. It is clear that from the results of this work the adsorption of mercury onto *Pterocarpus Anglolensis* is best described by the Freundlich isotherm. Furthermore, the linear and non-linear models of the Freundlich isotherm show good agreement. Therefore, Freundlich parameters can be used to describe the adsorption process. The value of $b_F$ (2.927 or 3.022) is higher than 1, which is an indication of minimal surface heterogeneity. As there is minimal heterogeneity the adsorption is most likely a multilayer process. Multilayer adsorption occurs mostly due to physisorption, whereby the heat of adsorption of the first layer is comparable to the heat of adsorption of the subsequent layer [43-44].

**Adsorption kinetics**

The experimental data were fitted to two models, pseudo-first-order kinetics and the pseudo-second-order kinetic models according to equations presented in Table 1.

***Table 2: Model parameters for Langmuir and Freundlich isotherms for adsorption of mercury onto Pterocarpus Anglolensis.***

| | Linear model | | | Non-linear model | | |
|---|---|---|---|---|---|---|
| Langmuir | $K_L$ (L/mg) | $a_L$ (L/μg) | $R^2$ | $K_L$ (L/mg) | $a_L$ (L/μg) | $R^2$ |
| | 0.039 | -0.028 | 0.985 | 0.165 | 0.000005 | 0.63 |
| Freundlich | $K_F$ (L/mg) | $b_F$ | $R^2$ | $K_F$ (L/mg) | $b_F$ | $R^2$ |
| | 0.0002 | 3.022 | 0.998 | 0.0003 | 2.927 | 0.998 |
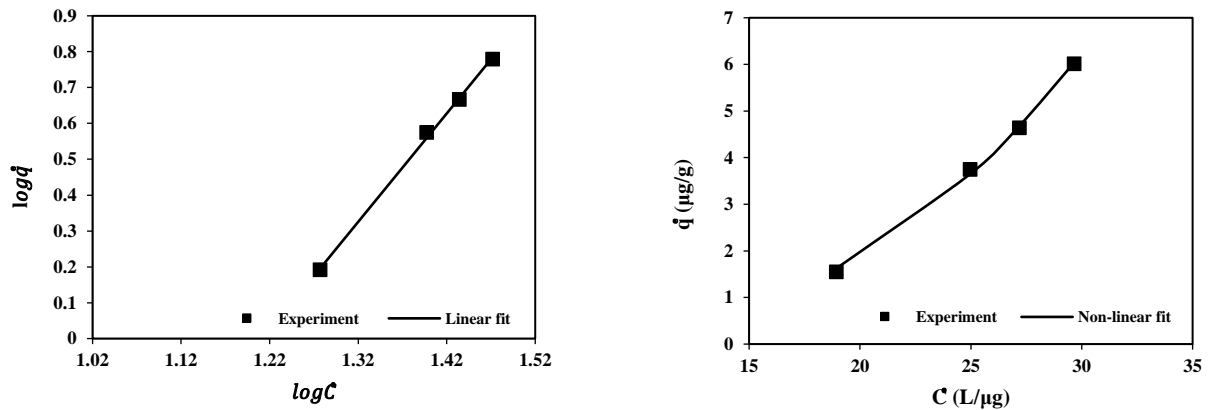


***Fig. 6: Freundlich plot for adsorption of mercury onto Pterocarpus Anglolensis [Agitation = 160 rpm, pH = 4, Particle size = 90 – 124 μm, Adsorbent mass = 1 g].***
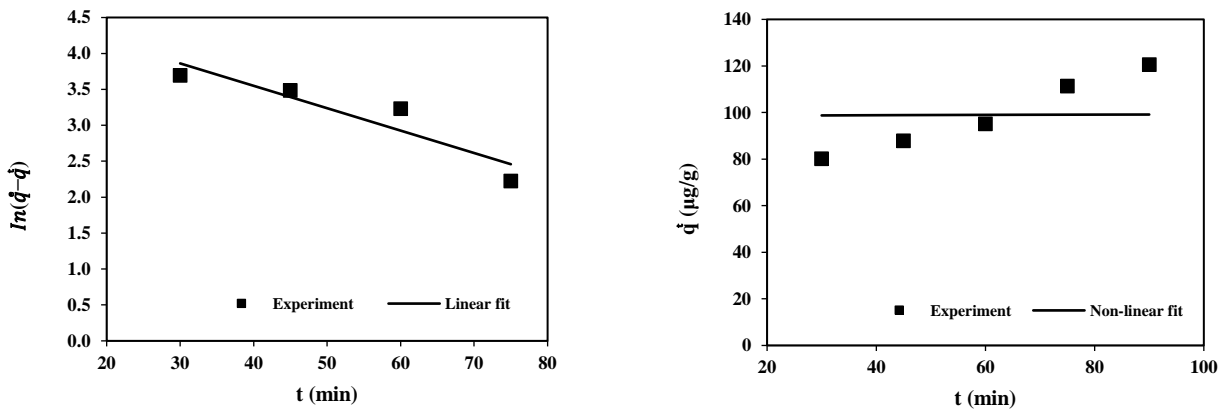


***Fig. 7: PFO kinetics plot for adsorption of mercury onto Pterocarpus Anglolensis [Agitation = 160 rpm, pH = 4, Particle size = 90 – 124 μm, Adsorbent mass = 1 g].***

These two models have been used to describe the kinetics of metal ion adsorption processes [23, 26]. Furthermore, linear and non-linear forms of the models were evaluated. The main contributing factors in adsorption are the structure of the adsorbent and the physical and chemical nature of solute and adsorbent.

Fig. 7 shows linear and non-linear PFO kinetics fits for the adsorption of mercury onto *Pterocarpus Anglolensis* sawdust. PFO kinetic model is based on the assumption of physisorption [45].

Fig. 8 shows linear and non-linear PSO kinetics fits for the adsorption of mercury onto *Pterocarpus Anglolensis* sawdust. PSO kinetic model is based on the assumption of chemisorption [45].

*Table 3: Model parameters for PFO and PSO kinetics for adsorption of mercury onto Pterocarpus Anglolensis .*

| | | | $k_1$ (min$^{-1}$) | $R^2$ |
|---|---|---|---|---|
| | | | 0.0177 | 0.018 |
| | | | $k_2$ (g/µg.min) | $R^2$ |
| | | | 0.00018 | 0.904 |

*Table 4: Comparison of isotherm and kinetics studies of different materials for the adsorption of mercury.*

| Adsorbent | Isotherm | Kinetics | Reference |
|---|---|---|---|
| *Pterocarpus Anglolensis* | Freundlich, linear, $K_F$ = 0.002 L/mg, $b_F$ = 3.022 | PSO, linear, $k_2$ = 0.0016 g/µg.min | This study |
| *Pterocarpus Anglolensis* | Freundlich, non-linear, $K_F$ = 0.003 L/mg, $b_F$ = 2.927 | PSO, non-linear, $k_2$ = 0.0018 g/µg.min | This study |
| Sulphur-coated magnetic carbon nanotubes | Langmuir, linear, $K_L$ = 0.516 L/mg | Not performed | [47] |
| *Borassus Flabeliffer* | Freundlich, linear, $K_F$ = 1.027 L/mg, $b_F$ = 1.478 | PSO, linear, $k_2$ = 0.299 g/µg.min | [48] |
| Mixed oxides nanoparticles | Sips, linear, $K_L$ = 0.516 L/mg | PSO, linear, $k_2$ = 0.00003 g/µg.min | [49] |
| Cassava peels modified with citric acid | Freundlich, non-linear, $K_F$ = 0.001 L/mg, $b_F$ = 2.069 | PSO, non-linear, $k_2$ = 0.067 g/µg.min | [50] |
| Lemon peels modified with citric acid | Freundlich, non-linear, $K_F$ = 1.908 L/mg, $b_F$ = 2.686 | PSO, non-linear, $k_2$ = 0.01 g/µg.min | [50] |
| Calcined sugar cane bagasse | Langmuir, linear, $K_L$ = 0.007 L/mg | PSO, linear, $k_2$ = 0.001 g/µg.min | [51] |
| Activated carbon from Walnut Shell | Langmuir, non-linear, $K_L$ = 0.009 L/mg | PSO, linear, $k_2$ = 0.00002 g/µg.min | [52] |
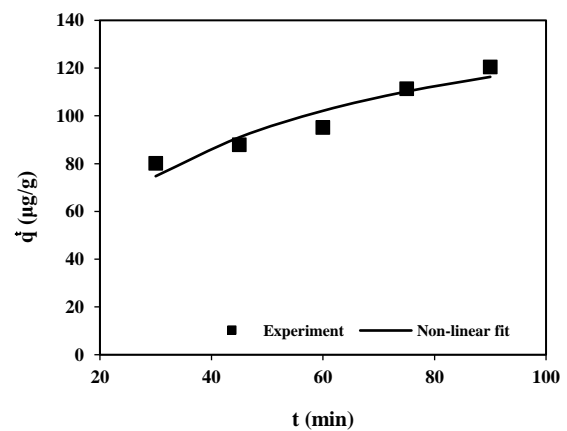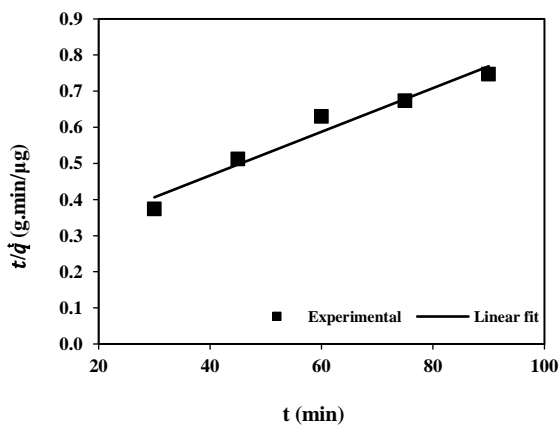


*Fig. 8: PSO kinetics plot for adsorption of mercury onto Pterocarpus Anglolensis [Agitation = 160 rpm, pH = 4, Particle size = 90 – 124 µm, Adsorbent mass = 1 g].*

The parameters of the PFO and PSO kinetic models are given in Table 3. It is clear that from the results of this work, the adsorption of mercury onto *Pterocarpus Anglolensis* is best described by PSO kinetics. The linear and non-linear models of the PSO model show good agreement. It has been suggested that the PSO model is suitable for low initial solute concentrations [46], nonetheless, results from this work suggest that the kinetics of mercury adsorption onto *Pterocarpus Anglolensis* fits the PSO reasonably well.

***Comparison of results with literature***

Several studies on the remediation of mercury from water have been conducted. Therefore, it is important to compare the results of this work with recent literature. Table 4 shows a comparison of this work's isotherm and

Research Article

kinetics study findings on adsorption of mercury with recent literature. It is clear from Table 4 that the adsorption of mercury onto the majority of low-cost adsorbents is described by the Freundlich isotherm and PSO kinetic model. Interestingly, the heterogeneity factors of the low-cost adsorbents displayed in Table 4 are all comparable.

**CONCLUSIONS**

A series of batch adsorption experiments were carried out to investigate the potential of *Pterocarpus Anglolensis* sawdust as an adsorbent for remediating water of mercuric contamination. Factors such as pH, contact time, and dosage influenced the adsorption and acidic conditions proved favorable. Isothermal studies were also conducted from the data obtained from the experiments and these, the Freundlich isotherm and Pseudo-second order kinetic model were best suited to describe the adsorption process. The overall outcome of the study managed to show that *Pterocarpus Anglolensis* sawdust has the potential in remediating water contaminated by mercury.

**REFERENCES**

[1] Jin-Gang Y., Bao-Yu Y., Xiong-Wei W., Qi L., Fei-Peng J., Xin-Yu J., Xiao-Qing C., Removal of Mercury by Adsorption: A Review, *Environ. Sci. Pollut. Res.,* **23(6)**: 5056-5076 (2015).

[2] Nour A., Ghadir E., Removal of Lead from Aqueous Solution Using Low Cost Abundantly Available Adsorbents, *Int. J. Environ. Sci. Tech.,* **4(1)**: 67-73 (2007).

[3] Diaz E., "Mercury Pollution at Gold Sites in the Amazon Environment", University of Idaho, Idaho (2000).

[4] Carvalho F.P., Mining Industry and Sustainable Development: Time for Change, *Food and Energy Security,* **6(2)**: 61-77 (2007).

[5] Morita M., Yoshinaga J., Edmonds J.S., The Determination of Mercury Species in Environmental and Biological Samples, *Pure Appl. Chem.,* **70(8)**: 1585-1615 (1998).

[6] van Straaten P., Mercury Contamination Associated with Small-Scale Gold Mining in Tanzania and Zimbabwe, *Sci. Total Environ.,* **259(1)**: 105-113 (2000).

[7] Miretzky P., Cirelli A.F., Hg(II) Removal from Water by Chitosan and Chitosan Derivatives: A Review, *J. Hazard. Mater.,* **167(3)**: 10-23 (2009).

[8] Lyons W.B., Wayne D.M., Warwick J.J., Doyle G.A., The Hg Geochemistry of a Geothermal Stream, Steamboat Creek, Nevada: Natural vs Anthropogenic Influences, *Environ. Geol.,* **34(1)**: 143–150 (1998).

[9] Mason R.P., Reinfelder J.R., Morel F.M.M., Uptake, Toxicity, and Trophic Transfer of Mercury in a Coastal Diatom, *Environ. Sci. Technol.,* **30(6)**: 1835–1845 (1996).

[10] Chen Z., Geng Z., Zhang Z., Ren L., Tao T., Yang R., Guo Z., Synthesis of Magnetic $Fe_3O_4$@C Nanoparticles Modified with $-SO_3H$ and $-COOH$ Groups for Fast Removal of $Pb^{2+}$, $Hg^{2+}$, and $Cd^{2+}$ Ions, *Eur. J. Inorg. Chem.,* **20(1)**: 3172–3177 (2016).

[11] Sibanda S., Nyoni B., Mpofu C., Naidoo B., Chiririwa H., Studying the Effectiveness of Treating Waste Water Using the Electro Coagulation Process at Sewage Treatment Plants, *Int. J. Appl. Chem.,* **13(4)**: 825-843 (2017).

[12] (a) Chiarle S., Ratto M., Rovatti M., Mercury Removal from Water by Ion Exchange Resins Adsorption, *Water Res.,* **34(11)**: 2971–2978 (2000).
(b) Lone S., Yoon D.H., Lee H., Cheong I.W., Gelatin-Chitosan Hydrogel Particles for Efficient Removal of Hg(II) from Wastewater, *Environ. Sci. Water Res. Technol.,* **5(1)**: 83-90 (2019).

[13] Han D.S., Orillano M., Khodary A., Duan Y., Batchelor B., Abdel-Wahab A., Reactive Iron Sulfide (FeS)-supported Ultrafiltration for Removal of Mercury (Hg(II)) from Water, *Water Res.,* **53(1)**: 310–321 (2014).

[14] Antochshuk V., Jaroniec M., 1-Allyl-3-Propylthiourea Modified Mesoporous Silica for Mercury Removal, *Chem. Commun.,* **3(2002)**: 258-259 (2002).

[15] Mirzababaei S.N., Taghizadeh M., Alizadeh E., Synthesis of Surfactant-Modified ZSM-5 Nanozeolite for the removal of Nickel (II) from Aqueous Solution, *Desalination Water Treatment,* **1**(2015): 1-12 (2015).

[16] Matlock M.M., Howerton B.S., Atwood D.A., Irreversible Precipitation of Mercury and Lead, *J. Hazard. Mater.,* **1**(2001): 73-82 (2001).

[17] Chiarle S., Ratto M., Rovatti M., Mercury Removal from Water by Ion Exchange Resins Adsorption, *Water Res.,* **34(11)**: 2971-2978 (2000).

[18] Zombrano J.B., Laborie S., Viers P.H., Rakib M., Durand G., Mercury Removal from Aqueous Solutions by Complexation-Ultrafiltration, *Desalination,* **144**(2002): 201-206 (2002).

[19] Mengdan X., Zhixin C., Yao L., Chuanhua L., Nasir M., Ahmad W., Cheema A., Shenmin Z., Removal of Hg(II) in Aqueous Solutions Through Physical and Chemical Adsorption Principles, *RSC Adv.,* **9**(2019): 20941-20953 (2019).

[20] Xu H., Xie J., Ma Y., Qu Z., Zhao S., Chen W., Huang W., Yan N., The Cooperation of Fe-Sn in a $MnO_x$ Complex Sorbent Used for Capturing Elementary Mercury, *Fuel,* **140**(2015): 803–809 (2015).

[21] Dube D., Champaklal C.T., Nyoni B., Removal of Chromium and Nickel from Electroplating Wastewater Using Magnetite Particulate Adsorbent: (1) Effect of pH, Contact Time and Dosage, (2) Adsorption Isotherms and Kinetics, *Modern Appl. Sci.,* **10(7)**: 222-232 (2016).

[22] Matthews T., Majoni S., Nyoni B., Naidoo B., Chiririwa H., Adsorption of Lead and Copper by a Carbon Black and Sodium Bentonite Composite Material: Study on Adsorption Isotherms and Kinetics, *Iran. J. Chem. Chem. Eng. (IJCCE),* **38(1)**: 101-109 (2019).

[23] Hossain M.A., Ngo H.H., Guo W., Introductory of Microsoft Excel SOLVER function-Spreadsheet for Isotherm and Kinetics Modelling of Metals Biosorption in Water and Wastewater, *J. Water Sustain.,* **3(4)**: 223-237 (2013).

[24] Gupta V.K., Carrott P.J.M., Carrott M.M.L.R., Low-Cost Adsorbents: Growing Approach To Wastewater Treatment –A Review, *Crit. Rev. Environ. Sci. Technol.,* **39(10)**: 783-842 (2009).

[25] Lopez-Luna J., Ramirez-Montes L.E., Martinez-Vargas S., Martinez A.I., Mijangos-Ricardez O.F., del Carmen A. González-Chávez M., Carrillo-González R., Solís-Domínguez F. A., del Carmen Cuevas-Díaz M., Vázquez-Hipólito V., Linear and Nonlinear Kinetic and Isotherm Adsorption Models for Arsenic Removal by Manganese Ferrite Nanoparticles, *SN Appl. Sci.* **1(950)**: 1-19 (2019).

[26] Nyoni B., Hlabano-Moyo B.M., Chimwe C., Using a Simulation Software to Perform Energy and Exergy Analyses of The Sulfur-Iodine Thermochemical Process, *Int. J. Model. Simul. Sci. Comput.,* **8(1)**: 1-14 (2017).

[27] Osmari T.A., Gallon R., Schwaab M., Coutinho E.B., Severo Jr J.B., Pinto J.C., Statistical Analysis of Linear and Non-Linear Regression for the Estimation of Adsorption Isotherm Parameters, *Adsor. Sci. Technol.,* **31(5)**: 433-458 (2013).

[28] Markovic D.D., Lekic B.M., Ognjanovic V.N.R., Onjia A.E., Rajakovic L.V., A New Approach in Regression Analysis for Modelling Adsorption Isotherms, *Sci. World J.,* **2014(1)**: 1-17 (2014).

[29] Yean S., Cong L., Yavuz C.T., Mayo J.T., Yu W.W., Kan A.T., Colvin V.L., Tomson M.B., Effect of Magnetite Particle Size on Adsorption and Desorption of Arsenite and Arsenate, *J. Mater. Resour.,* **20(12)**: 3255-3264 (2005).

[30] Abia A.A., Horsfall Jr M., Didi O., The use of Chemically Modified and Unmodified Cassava Waste for the Removal of Cd, Cu and Zn Ions from Aqueous Solution, *Bioresour. Technol.,* **90(3)**: 345-348 (2003).

[31] Horsfall Jr M., Abia A.A., Sorption of Cadmium(II) and Zinc(II) Ions from Aqueous Solutions by Cassava Waste Biomass (Manihot sculenta Cranz), *Water Res.,* **37(20)**: 4913-4923 (2003).

[32] Horsfall Jr M., Abia A.A., Spiff A.I., Removal of Cu (II) and Zn (II) Ions from Wastewater by Cassava (*Manihot esculenta* Cranz) Waste Biomass, *Afr. J. Biotechnol.,* **2(10)**: 360-364 (2003).

[33] Karabult S., Karabakan A., Denezli A., Yurum Y., Batch Removal of Copper (II) and Zinc from Aqueous Solution with Low Rank Turkish Coals, *Separat. Purif. Technol.,* **18**(2000): 177-184 (2000).

[34] Williams C.J., Aderhold D., Edyvean R.G.J., Comparison Between Adsorbents for the Removal of Metal Ions from Aqueous Solution, *Water Resour.,* **32**(1998): 216-224 (1998).

[35] Adouby K., Akissi K., Eboua L.C., Wandan N., Yao B., Removal of Heavy Metal Ions ($Pb^{2+}$, $Cu^{2+}$) in Aqueous Solutions by Pterygota Macrocarpa Sawdust, *J. Appl. Sci.,* **7(14)**: 1864-1872 (2007).

[36] Onwu F.K., Sonde C.U., Igwe J.D., Adsorption of Hg$^{2+}$ and Ni$^{2+}$ from Aqueous Solutions Using Unmodified and Carboxymethylated Granular Activated Carbon (GAC), *Am. J. Phys. Chem.,* **3**(**6**): 89-95 (2014).

[37] Abdelhamid B., Ourari A., Ouali M.S., Copper (II) Ions Removal from Aqueous Solution Using Bentonite Treated with Ammonium Chloride, *Am. J. Phys. Chem.,* **1**(2012): 1-10 (2012).

[38] Johnson R.D., Arnold F.H., The Temkin Isotherm Describes Heterogeneous Protein Adsorption, *Biochim. Biophys. Acta.,* **1247**(1995): 293-297 (1995).

[39] Kapoor A., Ritter J.A., Yang R.T., On the Dubinin-Radushkevich Equation for Adsorption in Microporous Solids in the Henry's Law Region, *Langmuir,* **5**(**4**): 1118-1121 (1989).

[40] Richardson J.F., Harker J.H., Backhurst J.R., (eds.), "Coulson and Richardson's Chemical Engineering, Particle Technology and Separation Processes", Vol. 2, 5th ed., Butterworth-Heinemann, Oxford, UK (2002).

[41] Jeppu G.P., Clement T.P., A Modified Langmuir-Freundlich Isotherm Model for Simulating pH-Dependent Adsorption Effects, *J. Contaminant Hydrol.,* **130**(**1**): 46-53 (2012).

[42] Christman K., "Introduction to Surface Physical Chemistry", Darmstadt, Steinkopf-Verlag (1991).

[43] Christmann K., "Thermodynamics and Kinetics Of Adsorption", University of Berlin (2012).

[44] Singha B., Das S.K., Adsorptive Removal of Cu(II) from aqueous Solution and Industrial Effluent Using Natural/Agricultural Wastes, *Colloids Surf. B: Biointerfaces,* **107**(**1**): 97–106 (2013).

[45] Azizian S., Kinetic Models of Sorption: A Theoretical Analysis, *J. Colloid Interface Sci.* **276**(**1**): 47-52 (2004).

[46] Fayazi M., Removal of Mercury(II) from Wastewater Using A New and Effective Composite: Sulfur-Coated Magnetic Carbon Nanotubes, *Environ. Sci. Pollut. Res.,* **2020**(**1**): 1-10 (2020).

[47] Kushwaha S., Sodaye S., Sadhakar P.P., Adsorption of Hg(II) from Aqueous Solution onto *Borassus Flabeliffer*: Equilibrium and Kinetic Studies, *Desalination Water Treatment,* **12**(2009): 100-107 (2009).

[48] Ashardi M., Nezhad A.K., Firouzabadi H., Abbaspourrad A., Adsorption of Mercury Ions from Wastewater by a Hyperbranched and Multi-Functionalized Dendrimer Modified Mixed-Oxides Nanoparticles, *J. Colloid Interface Sci.,* **505**(**1**): 293-306 (2017).

[49] Tovar C.T., Ortiz A.V., Jaraba L.E.G., Kinetics of Adsorption in Mercury Removal Using Cassava (*Manhiot esculenta*) and Lemon (*Citrus limonum*) Wastes Modified with Citric Acid, *Ing. Univ. Bogota (Colombia),* **19**(**2**): 293-298 (2015).

[50] Giraldo S., Robles I., Ramirez A., Florez E., Acelas N., Mercury Removal from Wastewater Using Agroindustrial Waste Adsorbents, *SN Appl. Sci.* **2**(2020): 1-17 (2020).

[51] Zabihi M., Haghighi Asl A., Ahmadpour A., Studies on Adsorption of Mercury from Aqueous Solution on Activated Carbons Prepared from Walnut Shell, *J. Hazard. Mater.,* **174**(**1**): 251-256 (2010).